

# Polar flocks with discretized directions: the active clock model approaching the Vicsek model

Swarnajit Chatterjee,<sup>1,\*</sup> Matthieu Mangeat,<sup>1,†</sup> and Heiko Rieger<sup>1,‡</sup>

<sup>1</sup>*Center for Biophysics & Department for Theoretical Physics,  
Saarland University, 66123 Saarbrücken, Germany.*

We consider the two-dimensional  $q$ -state active clock model (ACM) as a natural discretization of the Vicsek model (VM) describing flocking. The ACM consists of particles able to move in the plane in a discrete set of  $q$  equidistant angular directions, as in the active Potts model (APM), with an alignment interaction inspired by the ferromagnetic equilibrium clock model. We find that for a small number of directions  $2 < q \leq q_c = 5$  the flocking transition of the ACM has the same phenomenology as the APM, including macro-phase separation and reorientation transition. For a larger number of directions,  $q > q_c$ , the flocking transition in the ACM becomes equivalent to the one of the VM and displays micro-phase separation and only transverse bands, i.e. no re-orientation transition. Concomitantly also the transition of the  $q \rightarrow \infty$  limit of the ACM, the active XY model (AXYM), is in the same universality class as the VM. The main difference between the VM and the AXYM is the presence of a long range order at zero activity. We also construct an extensive coarse-grained hydrodynamic description for the ACM and AXYM akin to the VM.

Active matter consists of particles that consume energy and convert it, for instance, into directed motion. Being manifestly out of equilibrium active matter systems display novel many-particle effects or collective phenomena, like flocking, motility induced phase separation, giant number fluctuations, active turbulence etc. New models have been developed in the last two decades to understand and unravel the physical principles governing active matter systems [1]. The paradigmatic model for collective motion of animal groups, like bird flocks, buffalo herds, fish schools, is the Vicsek model (VM) [2], in which particles moving with constant velocity align their direction of motion with the average direction of their neighbors. At low noise and large density the VM displays a flocking transition to collective motion in a common direction. Subsequent studies showed that the way in which noise and disorder are introduced into the system [3, 4], range and type of the interactions [5–7] and alignment rules [8, 9] influence the characteristics of pattern formation and the type of phase transition occurring in Vicsek-like models.

Even the nature of the flocking transition of the original VM was debated for a long time: originally thought to be continuous [2] recent studies showed that it is discontinuous, reminiscent of a liquid-gas transition rather than a order-disorder transition [10]. In contrast to conventional first order phase transition scenarios, in which the system phase-separates macroscopically into a liquid and a gas phase in the coexistence region, the VM micro-phase separates into liquid bands of finite width moving coherently through the gas phase due to giant density fluctuations that break large liquid domains and arrest band coarsening [10]. Remarkably, such a micro phase

separation is absent in discretized versions of flocking models: the active Ising model (AIM) [11] as well as the  $q$ -state active Potts model (APM) [12] show macrophase separation in the coexistence region with only one liquid band moving in a gas background in a large aspect ratio rectangular geometry. In contrast to the VM, the APM displays additionally a reorientation transition from transversally moving bands for low particle velocities to longitudinally moving bands for high particles velocities [12].

A natural discretization of the VM (in 2d) is the 2d  $q$ -state active clock model (ACM), consisting of particles able to move in the plane in a discrete set of  $q$  equidistant angular directions, as in the AIM or APM, with an alignment interaction inspired by the ferromagnetic equilibrium clock model [13], approaching the ferromagnetic XY model in the limit  $q \rightarrow \infty$  [14]. Three questions arise in this context: 1) What is the nature of a putative flocking transition in the ACM for different values of the number of states  $q$ , regarding the fact that the equilibrium clock model has continuous BKT transition at a temperature  $T_{BKT}$  into a quasi-long range ordered phase and for  $q > 4$  another transition at a temperature  $T_{LRO} < T_{BKT}$  into a long-range ordered phase? [15] 2) If the transition is first order, what are the characteristics of the coexistence region: microphase separation as in the VM or macrophase separation as in the AIM and APM? Do longitudinally moving bands exist? 3) Is the  $q \rightarrow \infty$  limit of the ACM, the active XY model (AXYM) equivalent to the VM or does it remain macrophase separating as for finite  $q$ .

In this letter we will answer these question and will show that for a small number of states (directions)  $2 < q \leq q_c = 5$  the flocking transition of the ACM has the same phenomenology as the APM [12], including macro-phase separation and reorientation transition. For a larger number of states (directions),  $q > q_c$ , the flocking transition in the ACM becomes equivalent to the one of the VM and displays micro-phase separation and

\*Electronic address: swarnajit.chatterjee@uni-saarland.de

†Electronic address: mangeat@lusi.uni-sb.de

‡Electronic address: heiko.rieger@muni-saarland.de

only transverse bands, i.e. no re-orientation transition. Concomitantly also the transition of the AXYM is in the same universality class as the one of the VM. The letter is organized as follows: first we define the ACM in detail, then we present our numerical results and or hydrodynamic theory, and finally we discuss the implication of our findings.

**Model.** – The 2d  $q$ -state ACM consists of  $N$  particles moving in a rectangular domain of size  $L_x \times L_y$  with periodic boundary conditions and with average particle density  $\rho_0 = N/L_x L_y$ . Since no mutual exclusion among the particles are considered,  $\rho_0$  can assume values larger than 1. Each particle carries a clock degree of freedom or angle  $\theta \in \{0, 2\pi/q, 4\pi/q, \dots, 2(q-1)\pi/q\}$ , which also defines its preferred direction of motion in a biased diffusion. It can either jump to a new position or flip its angle. The hopping rate of a particle in state  $\theta$  in the (discrete) direction  $\phi$  is  $W_{\text{hop}} = D[1 - \varepsilon/(q-1)]$  for  $\phi \neq \theta$  and  $W_{\text{hop}} = D(1 + \varepsilon)$  for  $\phi = \theta$ , where  $D > 0$  is the diffusion constant and  $\varepsilon \in [0, q-1]$  is the bias, or “velocity”. Note that the total hopping rate is  $W_{\text{hop}}^{\text{tot}} = qD$  and that  $\varepsilon = 0$  corresponds to unbiased diffusion and  $\varepsilon = q-1$  to ballistic motion in the direction of the clock angle. If the hopping angle is  $\phi$  and we denote the position of the  $i^{\text{th}}$  particle at time  $t$  by  $\mathbf{x}_i(t)$ , then its position in the next time step is  $\mathbf{x}_i(t) + \mathbf{e}_\phi$ , where  $\mathbf{e}_\phi$  is the unit vector in  $\phi$ -direction. The flipping rate from  $\theta_i = \theta$  to  $\theta_i = \theta'$  is derived via detailed balance from a local clock Hamiltonian

$$H_i = -\frac{1}{2\rho_i} \sum_{k \neq l, k, l \in \mathcal{N}_i} \cos(\theta_k - \theta_l), \quad (1)$$

where  $\rho_i$  is the number of particles within its neighborhood  $\mathcal{N}_i = \{j \text{ with } |\mathbf{x}_i - \mathbf{x}_j| \leq 1\}$ :

$$W_{\text{flip}} = \gamma \exp \left\{ \frac{\beta J}{\rho_i} [\mathbf{m}_i \cdot (\mathbf{e}_{\theta'} - \mathbf{e}_\theta) + 1 - \cos(\theta - \theta')] \right\}, \quad (2)$$

where  $\mathbf{m}_i = \sum_{j \in \mathcal{N}_i} (\cos \theta_j, \sin \theta_j)$  is the local magnetization and  $\gamma$  is a constant.

For  $q = 4$  and  $6$ , one can define the ACM on square and triangular lattices, respectively, and identify the  $q$  different directions of motion to the  $q$  nearest neighbors. We analyzed these lattice versions, too, and obtained qualitatively identical results as those reported below [16], but here we restrict ourselves to the off-lattice version which allows a straightforward  $q \rightarrow \infty$  limit and is also closer to the original VM. In the limit  $q \rightarrow \infty$  the rescaled quantities  $\overline{D} = qD$  and  $\overline{\varepsilon} = \varepsilon/(q-1)$  have to stay finite and the angles become continuous with  $\theta \in [0, 2\pi]$ . The jump rate of a particle in state  $\theta$  in the (continuous) direction  $\phi$  becomes  $W_{\text{hop}} = \overline{D}(1 - \overline{\varepsilon})$  for  $\phi \in [0, 2\pi]$  and  $W_{\text{hop}} = \overline{D}\overline{\varepsilon}$  for  $\phi = \theta$ .

We performed Monte Carlo simulations of the  $q$ -state ACM and the AXYM, which evolve in discrete time steps of length  $\Delta t$ . In each time-step  $N$  (=number of particles) single particle updates are performed, one of which con-

sists in choosing randomly a particle which then either updates its spin state to  $\theta' \neq \theta$  chosen randomly with probability  $p_{\text{flip}} = W_{\text{flip}}\Delta t$ , or hops to one of the  $q$  directions with probability  $p_{\text{hop}} = \overline{D}\Delta t$ : in a random direction with probability  $(1 - \overline{\varepsilon})p_{\text{hop}}$  or in the direction  $\theta$  with probability  $\overline{\varepsilon}p_{\text{hop}}$ . The probability that nothing happens during this single particle update is  $p_{\text{wait}} = 1 - p_{\text{flip}} - p_{\text{hop}}$ . An expression for  $\Delta t$  can be chosen to minimize  $p_{\text{wait}}$ :  $\Delta t = [\overline{D} + \exp(2\beta J)]^{-1}$ . Without any loss of generality, we can take  $\overline{D} = 1$ ,  $J = 1$  and  $\gamma = 1$ .

We consider mainly a rectangular domain with a large aspect ratio with  $L_x = 400$  and  $L_y = 50$  for the computation of the phase diagram and other quantities.  $L_x = 800$  with varying  $L_y$  are considered for the snapshots presented. Simulations are performed for three control parameters: the noise is regulated by  $\beta = 1/T$ ,  $\rho_0 = N/L_x L_y$  defines the average particle density, and  $\overline{\varepsilon}$ , the self-propulsion parameter, dictates the effective velocity of the particles. The initial homogeneous system is prepared by assigning random initial position  $(x_i, y_i)$  and orientation  $\theta_i$  to each particle and then we let the system evolve under various control parameters for  $t_{\text{eq}} = 10^5$  to reach the steady-state. Following this, measurements are carried out with a maximum simulation time  $t_{\text{max}} = 20t_{\text{eq}}$ .

**Results.** – In Fig. 1(a) and Fig. 1(b), we show stationary density profiles for the  $q = 4$ -state ACM on a  $400 \times 50$  rectangular domain for fixed  $\beta = 2$  and  $\rho_0 = 1.5$  but for different bias: (a)  $\overline{\varepsilon} = 0.2$  and (b)  $\overline{\varepsilon} = 0.8$ . As observed before in the VM [2, 10], the AIM [11], and the  $q$ -state APM [12], the transition from a homogeneous gas phase to a polar liquid phase occurs through a liquid-gas coexistence phase, where a single band of polar liquid propagates on a disordered gaseous background. Akin to the 4-state APM [12], the band moves (a) transversally at small bias (velocity)  $\overline{\varepsilon} = 0.2$  and (b) longitudinal with respect to the band direction at larger bias  $\overline{\varepsilon} = 0.8$ . The coexistence phase in both figures shows a fully phase-separated density profile with a single *macroscopic* liquid domain as observed previously in the context of lattice flocking models [11, 12]. In Fig. 1(c) and Fig. 1(d), we display the temperature-density ( $T$ - $\rho_0$ ) phase diagram for  $\overline{\varepsilon} = 0.5$  and the velocity-density ( $\overline{\varepsilon}$ - $\rho_0$ ) phase diagram for  $\beta = 2$ , respectively. The liquid and gas binodals  $\rho_{\text{liq}}$  and  $\rho_{\text{gas}}$ , which segregate the gas-liquid (G+L) coexistence phase from the two homogeneous phases, liquid (L) and gas (G), are extracted from the time-averaged phase-separated density profiles. Reported for the first time in the context of the APM [12], we observe a similar reorientation transition of the coexistence phase from transverse band motion at low velocities and high temperatures to longitudinal lane formation at high velocities and low temperatures for  $q = 4$ . The physical origin of this reorientation transition, as argued in Ref. [12] with equivalent hopping rules, is the decrease of the transverse diffusion constant for large velocities, stabilizing the longitudinal lane formation. The reorientation transition occurs at  $\beta = 1.9$  (c) and  $\overline{\varepsilon} = 0.32$  (d), where the black

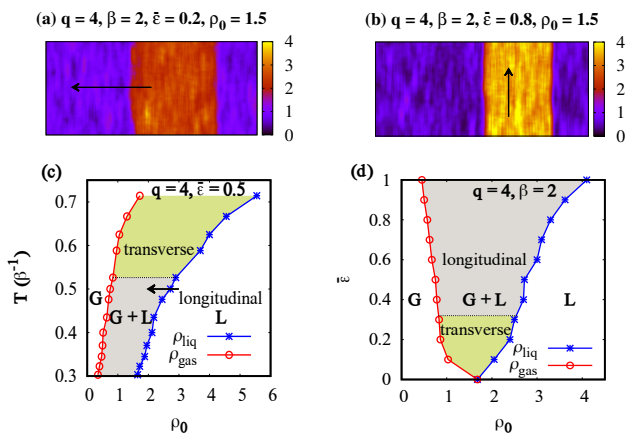


FIG. 1: (Color online) (a–b) Stationary density profiles for  $q = 4$ ,  $\beta = 2$  and  $\rho_0 = 1.5$  in a  $400 \times 50$  domain showing the bulk phase-separation and reorientation transition from (a) transverse band motion for  $\bar{\varepsilon} = 0.2$  to (b) longitudinal band motion for  $\bar{\varepsilon} = 0.8$ . The colorbar represents the particle density. (c) Temperature-density ( $T$ - $\rho_0$ ) phase diagram for  $\bar{\varepsilon} = 0.5$ , and (d) Velocity-density ( $\bar{\varepsilon}$ - $\rho_0$ ) phase diagram for  $\beta = 2$  of the  $q = 4$ -state ACM. The reorientation transition happens at  $\beta = 1.9$  and  $\bar{\varepsilon} = 0.32$ , respectively.

dotted lines delimit the two co-existing phase domains which are further marked by two distinct colors: grey for longitudinal lane motion and yellow for transverse band motion. We have obtained similar results from the numerical simulations of the 4-state ACM on a square lattice [16].

In Fig. 2(a) and Fig. 2(b), we show stationary density profiles for the  $q = 8$ -state ACM on a  $800 \times 20$  rectangular domain for  $\beta = 2$ ,  $\bar{\varepsilon} = 0.9$  and (a)  $\rho_0 = 1.5$  and (b)  $\rho_0 = 2$ . A *microphase* separation of the coexistence region, where periodically arranged ordered liquid bands move in the same direction in a gaseous background, is observed. The microphase-separated traveling bands are transverse in nature as observed first in the VM [2]. In a *microphase* separation, the traveling bands are not fully phase-separated and as established in Ref. [10], one crucial characteristic of this *microphase* separation is that the band number  $n_b$  increases with the density  $\rho_0$  as observed in Figs. 2(a)-(b). Time-averaged density profiles of the liquid-gas coexistence phase are shown in Fig. 2(c) which suggest that the width of the polar liquid band does not increase significantly with the average density  $\rho_0$ . We would like to briefly discuss the algorithm to obtain the time-averaged profiles. For each instantaneous density profile  $k$ , we first move the center of each of the  $n_b$  stripes to a fixed point  $x_0$  on the  $x$ -axis by doing a coordinate shifting (here  $x_0 = L_x/2$ ) and denote the averaged density over these stripes by  $\bar{\rho}_k(x)$ . We thermally average over  $n_p \simeq 200 - 300$  such instantaneous profiles and we finally obtain the time-averaged density profile as  $\langle \bar{\rho}(x) \rangle = \frac{1}{n_p} \sum_{k=1}^{n_p} \bar{\rho}_k(x)$ . It is well known that the band width does not affect the liquid ( $\rho_{\text{liq}}$ ) and the gas ( $\rho_{\text{gas}}$ ) binodals and we use this property to extract the relevant

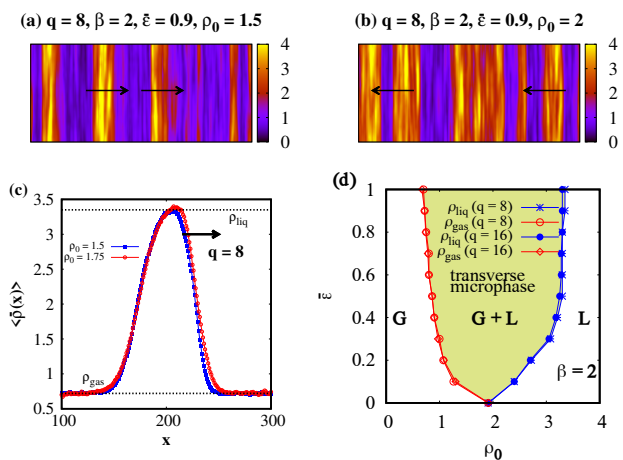


FIG. 2: (Color online) (a–b) Stationary density profiles for the  $q = 8$ -state ACM,  $\beta = 2$  and  $\bar{\varepsilon} = 0.9$  in a  $800 \times 20$  domain showing transversely moving microphase-separated bands for (a)  $\rho_0 = 1.5$  and (b)  $\rho_0 = 2$ . The colorbar represents the particle density. (c) Time-averaged density profiles for  $\rho_0 \in \{1.5, 1.75\}$  defining the two binodals  $\rho_{\text{liq}}$  and  $\rho_{\text{gas}}$ . (d) Velocity-density ( $\bar{\varepsilon}$ - $\rho_0$ ) phase diagrams for  $q = 8$  and  $q = 16$ -state ACM obtained for  $\beta = 2$  showing only transverse band motion.

phase diagrams. In Fig. 2(d), we represent the velocity-density ( $\bar{\varepsilon}$ - $\rho_0$ ) phase diagrams for  $\beta = 2$  and for  $q = 8$  and  $q = 16$ -state ACM. The two diagrams are very similar both qualitatively and quantitatively and implying a similar physical picture of the  $q$ -state ACM for  $q \geq 8$ . The corresponding coexistence domain is completely described by transversely traveling *microphase* separated bands. We would like to mention that although a reorientation transition occurs for  $q = 6$ -state ACM when simulated on a triangular lattice [16], we do not observe any reorientation transition for off-lattice simulations for  $q \geq 6$  at large bias  $\bar{\varepsilon}$  as observed for  $q = 4$ .

In Fig. 3(a) and Fig. 3(b), we present the stationary density profiles in the coexistence phase of the AXYM (i.e. for  $q = \infty$ ) on a  $800 \times 20$  rectangular domain and for  $\beta = 2$ ,  $\bar{\varepsilon} = 0.9$  and (a)  $\rho_0 = 1.5$  and (b)  $\rho_0 = 2$ . The AXYM and VM possess the same  $O(2)$  rotational symmetry but differ in their flipping and hopping rules. Nevertheless, we observe a *microphase* separation in the coexistence regime like in the VM [10] where the traveling bands are moving in the same direction and  $n_b$  is increasing with  $\rho_0$ . The temperature-density ( $T$ - $\rho_0$ ) and the velocity-density ( $\bar{\varepsilon}$ - $\rho_0$ ) phase diagrams are shown in Fig. 3(c) for  $\bar{\varepsilon} = 0.5$  and Fig. 3(d) for  $\beta = 2$ , respectively. We do not observe the reorientation transition akin to the observation made for  $q = 8$  and  $q = 16$ -state ACM. The velocity-density ( $\bar{\varepsilon}$ - $\rho_0$ ) phase diagram is again identical to Fig. 2(d) both qualitatively and quantitatively and thus minimizing the statistical errors in the calculations of the binodals, these three diagrams can be merged in a single diagram which signifies that the system behaves similarly for all large  $q$  values. The main

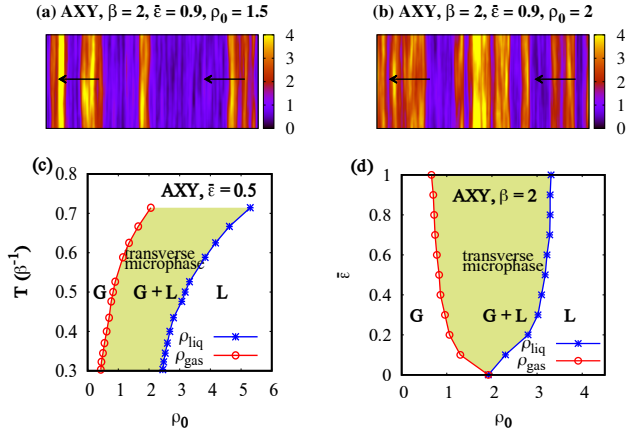


FIG. 3: (Color online) (a–b) Stationary density profiles for the AXYM,  $\beta = 2$  and  $\bar{\varepsilon} = 0.9$  in a  $800 \times 20$  domain showing transversely moving microphase-separated bands for (a)  $\rho_0 = 1.5$  and (b)  $\rho_0 = 2$ . The colorbar represents the particle density. (c) Temperature-density ( $T$ - $\rho_0$ ) phase diagram for  $\bar{\varepsilon} = 0.5$ , and (d) Velocity-density ( $\bar{\varepsilon}$ - $\rho_0$ ) phase diagram for  $\beta = 2$  for the AXYM showing only transverse band motion.

difference we observe between the VM and the AXYM is the nature of the  $\bar{\varepsilon} = 0$  transition at the density  $\rho_0 = \rho_*$  between a disordered and an ordered phase.  $\rho_*$  is the density for which the gas and liquid binodals at  $\bar{\varepsilon} = 0$  intersect in the velocity-density ( $\bar{\varepsilon}$ - $\rho_0$ ) phase diagrams (c.f. Fig. 3(d)), and it is identical with the unique density at which the Binder cumulant [17] does not depend on the system size [16]. For the VM, it was argued [10] that the critical point  $\rho^*$  is pushed to  $\rho^* = \infty$ , instead of a finite value  $\rho^* = 1.95$  as shown in Fig. 3(d). This difference between the zero-activity limits of the AXYM and the VM originates in the presence of particle diffusion in the AXYM, whereas particles in the VM are immobile in the zero-activity (=zero velocity) limit. For the  $q$ -state ACM and the AXYM we recover therefore the characteristic velocity-density ( $\bar{\varepsilon}$ - $\rho_0$ ) phase diagram observed in other discrete flocking models [11, 12].

In Fig. 4(a) and Fig. 4(b), we show the number fluctuations  $\Delta n^2 = \langle n^2 \rangle - \langle n \rangle^2$  and the magnetization fluctuations  $\Delta m^2 = \langle m^2 \rangle - \langle m \rangle^2$  for various  $q$  values, respectively.  $n$  and  $m$  are respectively the number of particles and the magnetization in boxes of different sizes  $\ell$  included in a  $100 \times 100$  domain (with  $\ell \leq 50$ ), with  $\langle n \rangle = \rho_0 \ell^2$ . The numerical simulation is performed in the liquid phase for  $\beta = 2$ ,  $\bar{\varepsilon} = 0.9$ , and  $\rho_0 = 6$ . As shown in Table I, both the fluctuations behave like  $\langle n \rangle^\xi$  with the same fluctuation exponent  $\xi$  increasing with  $q$ , from  $\xi \simeq 1$  for  $q = 4$  to  $\xi \simeq 1.67$  for large  $q$  (and saturates for  $q \geq 8$ ). Consequently the number and magnetization fluctuations show a transition from uniform fluctuations for small  $q$  to giant fluctuations at larger  $q$  as they have been observed in the VM [10]. These giant number fluctuations for large  $q$  are responsible for the microphase separation in the coexistence regime as

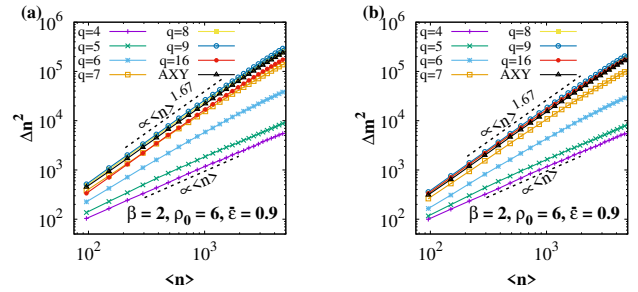


FIG. 4: (Color online) (a) Number fluctuations  $\Delta n^2 = \langle n^2 \rangle - \langle n \rangle^2$ , and (b) magnetization fluctuations  $\Delta m^2 = \langle m^2 \rangle - \langle m \rangle^2$  versus average particle number  $\langle n \rangle$  numerically calculated for  $\beta = 2$ ,  $\bar{\varepsilon} = 0.9$ ,  $\rho_0 = 6$ , and several  $q$  values in a  $100 \times 100$  square domain.

$q$	4	5	6	7	8	16	$\infty$
$\xi_n$	1.04	1.08	1.36	1.56	1.65	1.65	1.64
$\xi_m$	1.06	1.09	1.37	1.57	1.65	1.65	1.65

TABLE I: Number fluctuation exponents  $\xi_n$  and magnetization fluctuation exponent  $\xi_m$  for several values of  $q$ , reported from Fig. 4. The typical error on the fluctuation exponents is 0.01.

shown in Fig. 2(a–b) and Fig. 3(a–b) for  $q = 8$  and  $q = \infty$ , respectively. One can also observe that giant number fluctuations correspond to giant magnetization fluctuations or phase fluctuations which physically signifies weaker phase-ordering, and uniform number fluctuations correspond to smaller magnetization fluctuations which physically signifies stronger phase-ordering. Such a novel correspondence between the phase and density fluctuations has also been established in the context of a recent study [19] of diffusively mobile active XY spins where it has been argued that phase-ordering stronger or weaker than the quasi-long range order (QLRO) are accompanied by minuscule or giant number fluctuations, respectively.

**Hydrodynamic description.** – Next, we derive the main equations for the hydrodynamic continuum theory. From the microscopic hopping and flipping rates of the  $q$ -state ACM, we derive the master equation for the probability density function  $n(\mathbf{x}, \theta; t)$  for a particle to be at the position  $\mathbf{x}$  and in the spin-state  $\theta$  at the time [16]. We only keep the first-order terms in the  $|\mathbf{m}_i| \ll \rho_i$  expansion in the flipping rate (2). In the large system size limit  $L \gg 1$ , the hydrodynamic equation can be derived for the density  $\rho(\mathbf{x}; t) = \int d\theta n(\mathbf{x}, \theta; t)$  and the magnetization  $\mathbf{m}(\mathbf{x}; t) = \int d\theta \mathbf{e}_\theta n(\mathbf{x}, \theta; t)$ . Assuming the magnetization is a Gaussian variable with variance proportional

to  $\rho^\xi$ , as shown in Fig. 4, we obtain the equations [16]:

$$\partial_t \rho = D_0 \nabla^2 \rho + \frac{v}{4} \nabla \cdot (\nabla \cdot Q) - v \nabla \cdot \mathbf{m}, \quad (3)$$

$$\partial_t \mathbf{m} = D_0 \nabla^2 \mathbf{m} + \frac{v}{8} \begin{pmatrix} \partial_{xx} - \partial_{yy} & 2\partial_{xy} \\ 2\partial_{xy} & -\partial_{xx} + \partial_{yy} \end{pmatrix} \mathbf{m} - \frac{v}{2} (\nabla \rho + \nabla \cdot Q) + \gamma_0 \left[ \beta J - 1 - r \rho^\alpha - \kappa \frac{\mathbf{m}^2}{\rho^2} \right] \mathbf{m}, \quad (4)$$

with the diffusion constant  $D_0 = \bar{D}/4$ , the self-propulsion velocity  $v = \bar{D}\bar{\varepsilon}$ , the ferromagnetic interaction strength  $\gamma_0 = q\gamma/(q-1)$ ,  $\kappa = (\beta J)^2(7-3\beta J)/8$ ,  $\alpha = 2 - \xi$ , and the nematic tensor

$$Q = \frac{\beta J}{2\rho} \begin{pmatrix} m_x^2 - m_y^2 & 2m_x m_y \\ 2m_x m_y & -m_x^2 + m_y^2 \end{pmatrix}. \quad (5)$$

Note for  $r = 0$ , the simple mean-field theory can be recovered by neglecting the number and magnetization fluctuations. As shown in previous studies for the AIM and the APM [11, 12], these mean-field equations do not predict stable phase-separated profiles and will only give the trivial homogeneous solution. We note that (3-4) allow two homogeneous solutions with  $\rho = \rho_0$  corresponding to the gas phase:  $\mathbf{m} = \mathbf{0}$ , and the polar liquid phase:  $\mathbf{m}^2 = \rho_0^2(\beta J - 1 - r\rho_0^\alpha)/\kappa$ . The order-disorder transition at  $\bar{\varepsilon} = 0$  occurs at a density  $\rho_* = [(\beta J - 1)/r]^{1/\alpha}$ .

The Eqs. (3) and (4) are equivalent to the hydrodynamic equations derived for the VM [10, 20], although the second term of the right hand side of both equations is absent due to the biased diffusion present in the model. Applying the conclusions made in Ref. [10] to our hydrodynamic equations, we are not able to conclude when a macro-phase or a micro-phase separation is observed in the coexistence phase. Adding a zero-mean vectorial Gaussian white noise of variance  $\rho^\alpha(r - \kappa \mathbf{m}^2/\rho^\xi)$  to the Eq. (4) would be a possibility to scrutinize the stability of a macrophase or a microphase separation in the coexistence phase, as demonstrated for the VM in [10]. Moreover, the study of the existence of reorientation transition is feasible with Eqs. (3) and (4), as already done for the APM [12].

**Conclusion.** – The nature of the flocking transition in the  $q$ -state ACM and the AXYM is a liquid-gas phase transition for all values of the number of states  $q$ , similar to the VM [2, 10], the AIM [11] and the APM [12], with a coexistence phase delimiting the gas and liquid homogeneous phases. The coexistence phase shows a macrophase separation for  $q \leq 5$  as in the AIM and the APM, and

microphase separation for  $q \geq 6$  as in the VM. Longitudinally moving bands exist only when the coexistence phase is macrophase-separated, which implies that a re-orientation transition as in the APM [12] is absent for the ACM with  $q \geq 6$  and thus also for the AXYM, as it is for the VM. These results are supported by the number and magnetization fluctuations. Giant fluctuations observed for  $q \geq 6$  do not allow bulk phase separation and break large liquid domains into narrow periodic traveling bands and also restrict those bands from further coarsening, resulting in microphase separation.

Hence the discretization of the directions of motion in the VM as in the ACM will not change the characteristics of the VM flocking transition as long as the number of directions is sufficiently large ( $q \geq 6$ ). The main difference originates in the presence of a microscopic diffusive motion of particles in the ACM, leading to an order-disorder transition at  $\bar{\varepsilon} = 0$  and the presence of long-range order, which is absent in the VM. For a smaller number of directions ( $q < 6$ ) macro-phase separation and a re-orientation transition occurs. The hydrodynamic description that we derived for the  $q$ -state ACM is compatible with the hydrodynamic description for the VM presented in Refs. [10, 20], but is inconclusive regarding the stability of macro-phase or micro-phase-separation.

When this work was finalized we became aware of a related study [18] considering a version of the ACM/AXYM that differs in various important aspects from ours: in the model used in [18] 1) particles live on a square lattice and hence can only move in four different directions, 2) spin flips (clock changes) can only happen to the next hour and are 3) projected onto the four lattice directions, which is not fully commensurate with the spin anisotropy, 4) the hopping rules are defined differently, and 5) the hydrodynamic theory is one for XY spins in an anisotropy potential producing a term stabilizing LRO for all finite  $q$ -values, which is absent in our theory. As a consequence of these differences the predictions of [18] differ from ours and predict asymptotic macro-phase separation and the absence of a re-orientation transition for all  $q < \infty$ . Which one of the four aforementioned model differences is finally responsible for shifting  $q_c$  to infinity remains to be clarified in future work.

**Acknowledgement.** – This work was performed with financial support from the German Research Foundation (DFG) within the Collaborative Research Center SFB 1027. We want to thank Prof. Raja Paul for valuable discussions and for careful reading of the manuscript. SC and MM have contributed equally to the manuscript.

- 
- [1] M. R. Shaebani, A. Wysocki, R. G. Winkler, G. Gompper, and H. Rieger, *Computational models for active matter*, *Nature Reviews Physics* **2**, 181 (2020).  
 [2] T. Vicsek, A. Czirók, E. Ben-Jacob, I. Cohen, and O.

- Shochet, *Novel type of phase transition in a system of self-driven particles*, *Phys. Rev. Lett.* **75**, 1226 (1995).  
 [3] M. Aldana, V. Dossetti, C. Huepe, V. M. Kenkre, and H. Larralde, *Phase transitions in systems of self-propelled*

- agents and related network models, Phys. Rev. Lett. **98**, 095702 (2007).
- [4] F. Peruani and I. S. Aranson, *Cold active motion: How time-independent disorder affects the motion of self-propelled agents*, Phys. Rev. Lett. **120**, 238101 (2018).
- [5] F. Peruani, T. Klaus, A. Deutsch, A. Voss-Boehme, *Traffic jams, gliders, and bands in the quest for collective motion of self-propelled particles*, Phys. Rev. Lett. **106**, 128101 (2011).
- [6] F. Ginelli and H. Chaté, *Relevance of metric-free interactions in flocking phenomena*, Phys. Rev. Lett. **105**, 168103 (2010).
- [7] H. Chaté, F. Ginelli, G. Grégoire, F. Peruani, and F. Raynaud, *Modeling collective motion: variations on the Vicsek model*, Eur. Phys. J. B **64**, 451–456 (2008).
- [8] H. Chaté, F. Ginelli, and R. Montagne, *Simple model for active nematics: Quasi-long-range order and giant fluctuations*, Phys. Rev. Lett. **96**, 180602 (2006).
- [9] B. Mahault, X.-C. Jiang, E. Bertin, A.-Q. Ma, A. Patelli, X.-Q. Shi, and H. Chaté, *Self-propelled particles with velocity reversals and ferromagnetic alignment: Active matter class with second-order transition to quasi-long-range polar order*, Phys. Rev. Lett. **120**, 258002 (2018).
- [10] A. P. Solon, H. Chaté, and J. Tailleur, *From phase to microphase separation in flocking models: The essential role of nonequilibrium fluctuations*, Phys. Rev. Lett. **114**, 068101 (2015); A. P. Solon, J. B. Caussin, D. Bartolo, H. Chaté, and J. Tailleur, *Pattern formation in flocking models: A hydrodynamic description*, Phys. Rev. E **92**, 062111 (2015).
- [11] A. P. Solon and J. Tailleur, *Revisiting the flocking transition using active spins*, Phys. Rev. Lett. **111**, 078101 (2013); *Flocking with discrete symmetry: The two-dimensional active Ising model*, Phys. Rev. E **92**, 042119 (2015).
- [12] S. Chatterjee, M. Mangeat, R. Paul, and H. Rieger, *Flocking and re-orientation transition in the  $q$ -state active Potts model*, EPL **130**, 6 (2020); M. Mangeat, S. Chatterjee, R. Paul, and H. Rieger, *Flocking with a  $q$ -fold discrete symmetry: band-to-lane transition in the active Potts model*, Phys. Rev. E **102**, 042601 (2020).
- [13] J. V. José, L. P. Kadanoff, S. Kirkpatrick, and D. R. Nelson, *Renormalization, vortices, and symmetry-breaking perturbations in the two-dimensional planar model*, Phys. Rev. B **16**, 1217 (1977); J. L. Cardy, *General discrete planar models in two dimensions: Duality properties and phase diagrams*, J. Phys. A **13**, 1507 (1980); M. S. S. Challa and D. P. Landau, *Critical behavior of the six-state clock model in two dimensions*, Phys. Rev. B **33**, 437 (1986); S. K. Baek, P. Minnhagen, and B. J. Kim, *True and quasi-long-range order in the generalized  $q$ -state clock model*, Phys. Rev. E **80**, 060101(R) (2009).
- [14] J. M. Kosterlitz and D. J. Thouless, *Ordering, metastability and phase transitions in two-dimensional systems*, J. Phys. C **6**, 1181 (1973); J. M. Kosterlitz, *The critical properties of the two-dimensional XY model*, J. Phys. C **7**, 1046 (1974).
- [15] S. Chatterjee, S. Puri, and R. Paul, *Ordering kinetics in  $q$ -state clock model: scaling properties and growth laws*, Phys. Rev. E **98**, 032109 (2018); Z.-Q. Li, L.-P. Yang, Z.-Y. Xie, H.-H. Tu, H.-J. Liao, and T. Xiang, *Critical properties of the two-dimensional  $q$ -state clock model*, Phys. Rev. E **101**, 060105 (2020).
- [16] See the Supplementary Material.
- [17] K. Binder, *Finite Size Scaling Analysis of Ising Model Block Distribution Functions*, Z. Phys. B **43**, 119 (1981).
- [18] A. Solon, H. Chaté, J. Toner, and J. Tailleur, *Susceptibility of Polar Flocks to Spatial Anisotropy*, arXiv:2201.00704v2 (2022).
- [19] A. Haldar, A. Sarkar, S. Chatterjee, and A. Basu, *Active XY model on a substrate: Density fluctuations and phase ordering*, arXiv:2105.03919v3 (2021).
- [20] J. Toner and Y. Tu, *Long-Range Order in a Two-Dimensional Dynamical XY Model: How Birds Fly Together*, Phys. Rev. Lett. **75**, 4326 (1995); J. Toner and Y. Tu, *Flocks, herds, and schools: A quantitative theory of flocking*, Phys. Rev. E **58**, 4828 (1998).